University of Dundee

Semi-automatic lymph node segmentation and classification using cervical cancer MR imaging

Bnouni, Nesrine; Mechi, Olfa; Rekik, Islem; Rhim, Mohamed Salah; Ben Amara, Najoua Essoukri

Semi-Automatic Lymph Node Segmentation and Classification using Cervical Cancer MR Imaging

Nesrine Bnouni[1], Olfa Mechi[1], Islem Rekik[2], Mohamed Salah Rhim[3], Najoua Essoukri Ben Amara[1]

[1]LATIS– Laboratory of Advanced Technology and Intelligent Systems, ENISo, Sousse University
[2]BASIRA lab, CVIP group, School of Science and Engineering, Computing, University of Dundee, UK
[3]Department of Gynecology Obstetrics, Faculty of Medicine of Monastir, Tunisia
Email: nesrine.bnouni@gmail.com

Abstract—**The segmentation and classification of Lymph Nodes (LNs) is a fundamental but challenging step in the analysis of medical images of cervical cancer. Both tasks can leverage morphological features such as size, shape, contour, and heterogeneous appearance. However, these features might vary with the progressive state of LNs. Hence, accurate detection of LNs boundary is an essential step sing to classify LN as suspect (malignant) and non-suspect (benign). However, manual delineation of LNs might produce classification errors due to the inter and intra-observer variability. Semi-automatic and automatic LNs segmentation methods are greatly desired as they would help improve patient diagnosis and treatment processes. Currently, Magnetic Resonance Imaging (MRI) is widely used to diagnose cervical cancer and LN involvement. Diffusion Weighted (DW)-MRI exhibits metastatic LN as bright regions. This paper presents a semi-automatic *segmentation* and *classification* method of LNs. Specifically, we propose a novel approach which leverages (1) the complementarity of structural and diffusion MR images through a fusion step and (2) morphological features of the segmented metastatic LNs for classification. The contribution of our proposed algorithm is threefold. *First*, we fuse the axial T2-Weighted (T2-w) anatomical image and the DW image. *Second*, we detect LNs using region-growing method in order to compute the final classification. *Third*, segmentation results are then used to classify LNs based on a gray level dependency matrix technique which extracts LN features. We evaluated our method using 10 MR images T2-w and DW with 47 metastatic LNs. We obtained an average accuracy of 70.21% for cervical cancer nodule classification.**

Keywords—lymph nodes; cervical cancer; segmentation; classification; multimodal image fusion; MR imaging; abnormal node detection

I. INTRODUCTION

Cervical carcinoma is the second mostly common gynecological malignancy in the world [1]. It is a slowly growing disease, mostly invading the vagina, the parametrium and the uterosacral ligaments. In later stages, the bladder, the rectum and the pelvic and para-aortic Lymph Nodes (LNs) can be invaded. LN involvement is well known as a wicked prognosis factor in cervical cancer. LN is an oval-shape organ of the immune system, which is difficult to identify in most cases and is widely distributed throughout the body. Enlarged LNs are defined by the widely observed RECIST criterion [2] to have signaled the onset or progression of a malignant disease or an infection. Classifying LNs into suspect and non-suspect depends on the radiologist's experience. In fact, morphological features such as size, shape, contour, and heterogeneous appearance help improve the detection of metastatic LNs. Extracting these morphological features in an automated way while avoiding errors due to the inter and intra-observer variability would much facilitate staging and patient diagnosis for clinicians. Often carried out by hand, the segmentation of LNs can be tedious, highly complex and time-consuming. Hence, semi-automatic and automatic LNs segmentation methods are highly desired as they can decrease variability in classification results by multiple experts and speed up the diagnosis process. Magnetic Resonance Imaging (MRI) of the pelvis is actually considered as the gold standard for staging and treatment planning of cervical cancer. While, MRI has high contrast and spatial resolution for pelvic organs and tissues, Diffusion Weighted (DW)-MRI displays metastatic LN as bright regions [3]. Leveraging the complementary aspects of both T2-Weighted (T2-w) and DW imaging modalities, we propose a new method to fuse the axial T2-w anatomical sequence and the diffusion sequence. Next, we segment LNs using region-growing algorithm. With the fusion of both T2-w and DWI imaging modalities, the unique characteristics provided by each modality is combined.

Image fusion techniques have gained popularity in medical image analysis, such as MRI-ultrasound fusion to improve prostate cancer detection [4, 5]. Several previous works have targeted the detection of LNs, including atlas-based segmentation for head-and-neck cancer [6], the 3D mass-spring models for the segmentation of neck LNs in Computed Tomography (CT) datasets [7], and the statistical image feature learning [8]. In [9], the authors decomposed 3D into 2D convolutional neural networks by randomly sampling them for the detection of LNs. Nogues et al. [10] used a new approach to joint holistically-nested neural networks to the structured optimization for automatic LN segmentation. In [11], the authors utilized an automatic method that would detect chest LNs in 3D CT image data. Zhang et al. [12] used a new deep learning method for automatically segmenting LNs in

ultrasound images. In [13], a novel method that combined the graph cut with locally adaptive energy was used for segmentation of human LNs in ultrasound images. Although promising, all these methods did not exploit DW image where metastatic LN (i.e., suspect) have a higher intensity than that of a benign LN (i.e., non-suspect). This paper addresses this limitation by proposing a T2-w and DW image fusion step for LN segmentation and classification. Moreover, to the best of our knowledge, this presents the first work that aims to detect and stratify LN in *cervical cancer*. Section 2 introduces the LN problem and our proposed method. All the details of the MRI and DWI fusion, LN segmentation and classification steps are described in sections 3, 4 and 5, respectively. Finally, section 6 describes the results of our approach, and section 7 concludes the paper.

II. LYMPH-NODE

A. Pelvic Lymph Nodes

Pelvic LNs are part of the lymph system, which carries fluid, nutrients, and waste material between the body tissues and the bloodstream. LNs are connected by a system of channels that runs throughout the body. Cancer may spread through the LNs to distant parts of the body. LNs need to be considered during the oncological examination related to all types of cancer, for instance cervical one, where metastasis settles in the LNs. The LNs will gradually reduce in size and come to the normal size when the cancer treatment is efficient.

B. Computer Aided Approach

For LN segmentation and classification, we first propose a semi-automatic computer-aided approach to extract morphological features and classify them. The first step is *fusion* of T2-w and DW-MR images. The second one is LN *segmentation*. Specifically, we use segmentation to divide the image into two different regions of interest: LN and non-LN regions. This step results in a 2D binary mask for the LNs. Third, we utilize both the Gray Level Dependency Matrix (GLCM) technique and the generated mask to extract morphological features from the detected LNs. Next, a decision tree-based classification model uses the features obtained from the GLCM result to differentiate between a suspect and non-suspect LN, as illustrated in Fig. 1. Our proposed block diagram contains three phases: (1) fusion, (2) segmentation, and (3) classification. These steps will be detailed in what follows.

III. FUSION

Image fusion has gained popularity in medical diagnosis and treatment [14]. It is utilized when multiple images of a patient are registered or merged to provide additional information. Fused images may be estimated from multiple images from the same imaging modality [15] or from multiple modalities [14]. The fusion image is used to obtain more discriminative morphological feature (the intensity of the fused image in order to use both the T2 axial and DW image intensity criterion) for the verification stage. In our case, two different imaging modalities including axial T2-w and DW images are used.
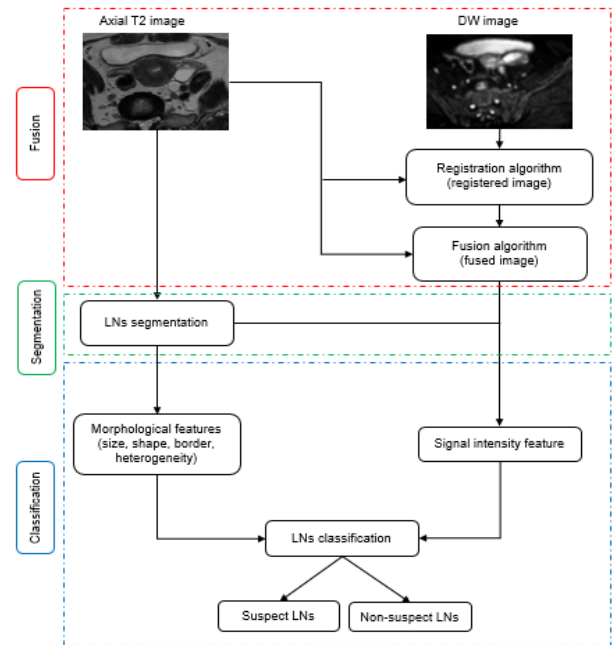

Fig.1. Flowchart of the proposed LN segmentation and classification. In the fusion step, we fuse both axial T2-w and DW modalities for each patient. Then, we generate the LN segmentation mask using T2-w images and region-growing algorithm. We use the same mask to segment LNs in fused images. Next, we extract several morphological features from the segmented LN to classify them as suspect or non-suspect.

A. Axial T2-2 Image

For LN classification, we use the axial view of T2-w image (Fig. 2).

B. DW Image

The DW imaging contrast is based on the differences in the water-proton mobility between tissues. In addition to that, it reflects tissue cellularity and wholeness membrane cellularity. Tumor tissues are more cellular compared with the native tissues from which they originate, and they show a high signal on the DW-MR imaging. The latter improves the detection of LNs. Fused images created by the addition of the DW-MR imaging to a conventional T2 image can improve the detection of small LNs throughout the body. Early reports utilizing DW imaging for the identification of malignant nodes in patients having cervical cancers have been encouraging. DW imaging is very useful for LN detection. Both DW and T2-w MRI are commonly used for the detection and evaluation of an LN metastasis, where the intensity in the LN metastasis is higher than in the benign LN. Hence, we aim to fuse both T2-w and diffusion to improve the diagnostic accuracy of the MRI (Fig. 3). To obtain fused images,
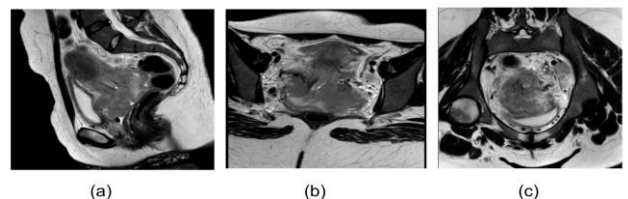

Fig.2. T2-w image contains 3 sequences: (a) sagittal, (b) axial and (c) coronal images. For LN segmentation and classification, we use axial T2-w image.
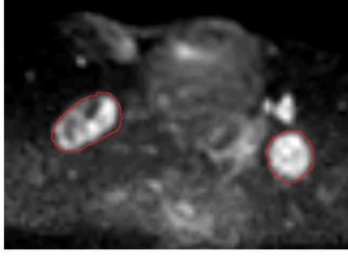
Fig.3. DW-MR Image: DW-MRI with segmentation of malignant LNs (outlined in red). In a DW image, malign LNs appear with a high intensity compared to benign LNs, hence the advantage of using this sequence in LN segmentation.

we first register the DW image space to the axialT2-w image space.

C. Image Registration

Image registration is commonly used for medical image analysis to aligh high-dimensional data to a common space. There exist two transformation models of registration methods. The first model includes affine and rigid transformation. The second includes a non-rigid transformation. In this work, we use non-rigid transformation method. The choice of this method is based on a comparative study with the rigid transformation, based on the Dice coefficient, the mutual information criteria and the distance between the centers of the segmented masses to judge the quality of the registred image. For the distance measure, the Euclidean distance between the centers of the segmented LNs from the reference image and the registered one is computed. The Dice coefficient is defined as in (1):

$$Dice = 2(A \cap B)/(A + B) \qquad (1)$$

where A indicates the ground truth segmentation map and B the estimated label map. We also use mutual information for assessing registered image quality, defined as follows (2):

$$MI(A, B) = H(A) + H(B) - H(A, B) \qquad (2)$$

where H(A) and H(B) denote the marginal entropies, and H(A,B) is the joint entropy of A and B.

We use two types of pelvic MRI images: T2-w and DW. We fix T2-w image as a reference and move DW image to T2-w image space. These two images have different intensity distributions, so we use a multimodal registration. The histogram in Fig. 4 shows that we obtain a better result by using non-rigid registration. Examples in Fig. 5 show how we can use image registration to automatically align two MR modalities to a common coordinate system through utilizing image registration technique [16]. In this case, a non-rigid transformation of DW image is obtained. This will be used for fusing DW image with T2-w image to infer the most comprehensive information than provided by either.

D. Image Fusion

For image fusion, we use the wavelet-based fusion technique, as it is suitable for fusion when a multi-view image
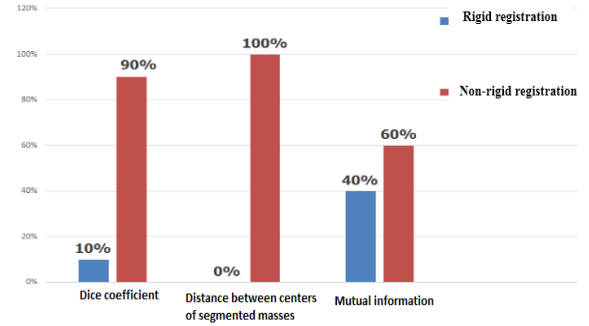

Fig.4. Histogram of comparison between two types of registration (rigid and non-rigid) on all LNs. We obtained a better result by using the non-rigid registration.

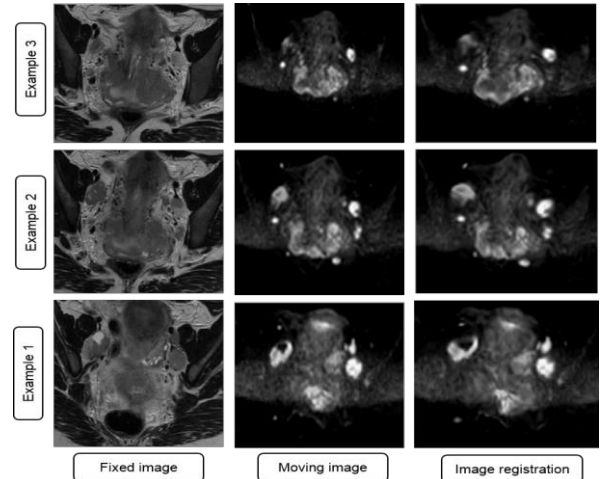Fixed image   Moving image   Image registration

Fig.5. Two types of pelvic MRI images are used: T2-w axial and DW Image. The fixed image is the axial T2-w image, and the moving image is the DW image.

fusion required to be done. Wavelet-based fusion technique uses the discrete wavelet transform that can provide the best spectral and spatial localization of image information [17]. It can also extract coarse-to-fine details from images to fuse. The resulting fused image can have reliable characteristics in terms of features from both images, which improves the quality of imaging [14]. Fig. 6 shows an example of our fusion image process. Subsequently, we locate LNs and their boundaries firstly in the T2-w images using region-growing algorithm. Then, we use the same segmentation for fused images in order to extract LN features and classify them afterwards. It is supposed that, after registration, the LNs in T2 axial images and LNs in DW registered images have the same LN segmentation.

IV. LYMPH-NODE SEGMENTATION

LN segmentation plays a crucial role in important medical-imaging-based diagnosis tasks, such as the quantitative evaluation of disease progression or the effectiveness of a given treatment or therapy. LN are often textured in complex ways; however, they are presented as contiguous regions. Thus, we propose to use a region-growing technique for segmentation. Region growing is a process of segmentation of images based on regions. It is a pixel-based image segmentation way.
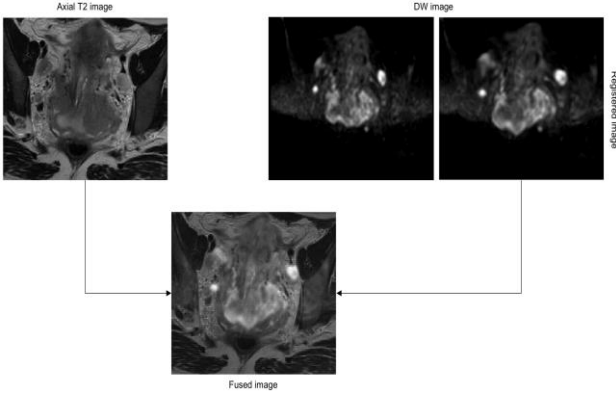
Fig.6. Multimodal MR fusion image: The fused image is obtained by combining information from the DW registered image and the T2-w MRI image in order to produce an image that integrates complementary information from both modalities.

Specifically, this approach iteratively analyzes the neighboring initial-seed-point pixels and determines whether the pixel neighbors ought to be added to the region. It has been used for several segmentation tasks including retinal-vessel segmentation [18], vessel-segmentation algorithm based on spectrum information [19], and color image segmentation and for segmentation of synthetic aperture radar [20,21].

In order to start the region-growing algorithm, we select at first an initial seed point in the axial slice of the LN part. Following the extraction of one region, the procedure of region growing is iterated. We compute a coronary mask from an LN based region-growing algorithm. Whereas, thresholding and region-growing approaches utilize intensity based criteria. Finally, we compare the size and the number of segmented LN regions in an axial direction with manual segmentation. Once the LN region is segmented, we then classify it as metastatic or benign according to the LN malignancy criteria.

V. LYMPH-NODE CLASSIFICATION

A. Criteria for Normal and Abnormal Nodes in Cervical Cancer on MR Imaging

The LN involvement is a prognostic value of cervical cancer and consequently influences the choice of therapy. Table I states the morphological MRI criteria that can be useful for nodal assessment and classification in cervical cancer.

TABLE I.   MORPHOLOGICAL MRI CRITERIA FOR SUSPECT AND NON-SUSPECT NODES IN CERVICAL CANCER

Nodal Criteria	Normal	Abnormal
Nodal size	≤ 8mm	> 8mm
Nodal shape	Elliptical	Round
Nodal contour	Regular	Irregular
Nodal appearance	Homogenous	Heterogeneous

This section recapitulates the features used in our approach. We define five features in this study. Four morphological features are extracted from the axial T2 MR image (node size, node shape, node contour and node heterogeneity) and the relative signal intensity is extracted from the fused image.

1) Size: The nodal size is the most important criterion utilized to differentiate benign from metastatic nodes. However, the nodal size alone cannot be used to distinguish benign from metastatic LNs [22]. In agreement with the late RECIST criteria [2], pathologic nodes, having the identity known as target lesions, have to cope with the criterion of a short diameter axis of not less than 10 mm on MRI. If this axis is more than 1 cm, the LNs will be considered suspect. In cervical cancer, LNs larger than 8 mm are considered suspect, with a significant diagnostic sensitivity and specificity compared with conventional imaging. Fig. 7 shows LN metastasis with a 41.2-mm long axis diameter, and 20.9-mm short axis diameter, respectively.

2) Shape: The LN has a blob shape. Benign nodes are more probable to be ovoid and they become more round due to malignant infiltration. Furthermore, if the ratio of the long-axis diameter to the short-axis one is less than 2 as in (3), then the LN is more likely to be malignant [23].

$$\frac{Long\ axis}{Short\ axis} < 2 \qquad (3)$$

Even though the round shape aids in identifing metastatic LN, it cannot not be utilized as an exclusive criterion of nodal assessment on account of round parotid and normal submandibular nodes [23].

3) Contour: The nodal MR-imaging contour may have a larger discriminatory value. Added to that, some malignant nodes demonstrate irregular borders as a result of the extracapsular disease extension. Metastatic LNs are characterized by ill-defined borders, while benign LNs show well-defined borders [22]. The sharp border in the metastatic nodes is caused by the existing intranodal tumor infiltration that increases the acoustic impedance difference between surrounding and intranodal tissues. Therefore, the nodal border alone cannot be a criterion worthy of being depended on to distinguish normal nodes from abnormal ones in a routine clinical practice. Nevertheless, the appearance of an ill-defined boundary is helpful in predicting patient diagnosis. Energy measure from GLCM is used to calculate border values. It is measured according to (4):

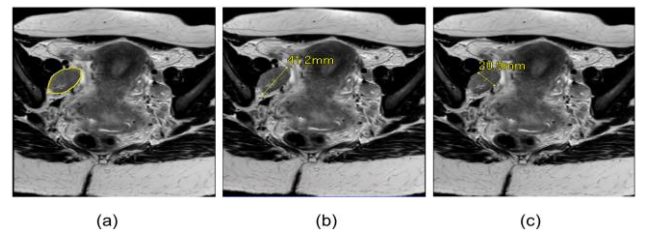$$\sum_{(i,j)} p(i,j)^2 \qquad (4)$$

Fig.7. LN size example: (a) LN segmentation outlined in yellow, (b) 41.2mm long axis diameter, (c) 20.9mm short axis diameter.

The energy yields the sum of squared elements in the GLCM and returns a value between 0 and 1. If the value is greater than 0.7, the contour is considered regular.

4) Appearance: We define the LN heterogeneity index (H) as in (5):

$$H = - \sum_i P(i) \log[P(i)] \qquad (5)$$

where (H) is the theoretic entropy of the selected region and P(i) is the histogram of intensity values of the selected inner region. It relatively has low values every time that the histogram is precipitously peaked, which indicates that the signal is homogeneous. On the other hand, it will have relatively high values in case the histogram is widely spread, which shows that the signal is heterogeneous.

5) Intensity: Tumor tissues have higher signals on the DW-MR image compared with natural tissues. In addition, they have an intermediate signal on the T2-w. Thus, we fuse T2 axial and DW images and we calculate the mean signal intensity (GLCM) for each LN.

VI. RESULTS

A. LN Segmentation Results

1) Dataset description. We carryied out the experiments on 10 T2-w and DW pelvic cervical cancer MRI images with 54 metastatic LNs segmented by an expert radiologist. We note that DW image is smaller than T2 axial image. We also note that the DW image corresponding to the T2 axial image were provided by an expert.

2) Parameter setting and evaluation. The accuracy of the segmentation is calculated using the average Dice coefficient (± standard deviation) according to equation (1) where A represents the ground truth and B the results using the region growing approach.

In this work, we used region-growing for LN segmentation (Fig. 8). Fig. 9 displays our semi-automatic LN segmentation results along with ground-truth segmentation for 3 representative subjects. We calculated the Dice coefficient using the 10 manually labeled images to evaluate the correspondence between region-growing segmentation and a human-rater segmentation. The detailed experimental results are reported in Table II. We used the results of LN segmentation to further classify each segmented LN as suspect or non-suspect. Undoubtedly, the segmentation results affect the classification results.

TABLE II.   SEGMENTATION RESULTS

Mean Dice	70.68%
Standard deviation	14.59%

B. LN Classification Results

Table III summarizes the experiment of our method. We obtained a better result by adding the criterion of the intensity of the merged image. The combination of morphological and fusion features boosted the segmentation accuracy up to 70.21%, in comparison to 63.82% obtained when solely using morphological features (size, shape, contour and heterogeneous appearance). The integration of the fusion features into the algorithm improved the diagnostic accuracy. In our experiment, we found the same result using the intensity of the fused image compared to when using the intensity of registered DW image. Our proposed method significantly (p<0.05) outperformed morphological feature-based classification method (without fusion features) and produced the best classification accuracy. We note that we did not post-process the tumor boundary outputted by region-growing segmented method. Furthermore,
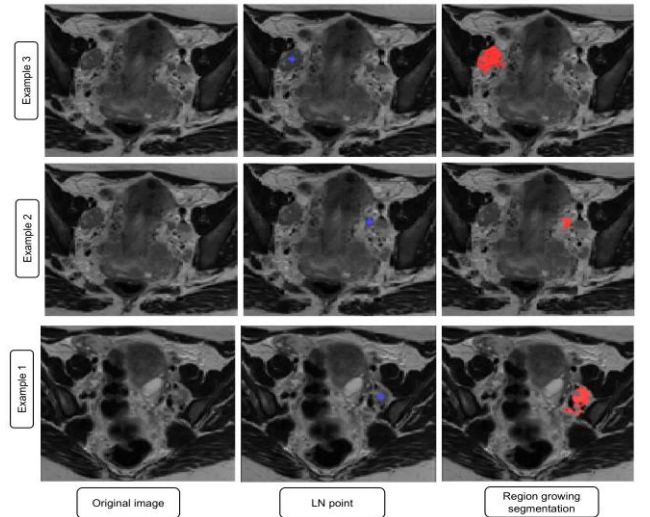

Fig.8. Semi-automatic LN segmentation: One point in axial slice of the LN part was determined. Then, we apply region-growing algorithm for segmentation of the LNs.
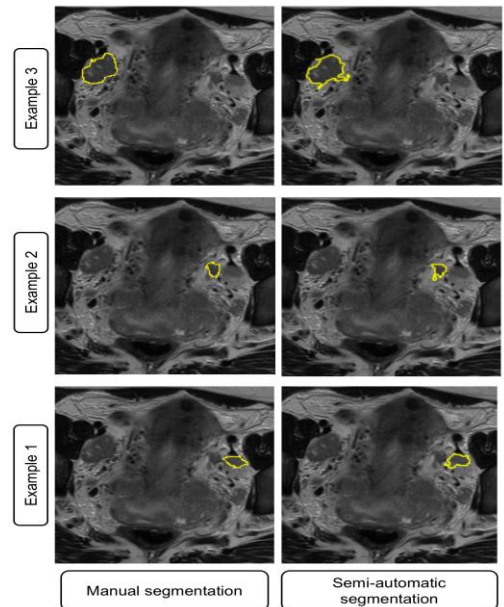

Fig.9. LN segmentation results for three representative subjects using our proposed method (right column) and manual segmentation by expert radiologist (left column).

the registration and segmentation results immediately affect the performance of LN classification.

TABLE III. CLASSIFICATION RESULTS

Features Used for Classification	Number of Detected LNs	Percentage
Morphological features	29/47	63.82%
(Morphological + Diffusion) features	33/47	70.21%
(Morphological + Fusion) features	33/47	70.21%

VII. CONCLUSION

Lymph nodes play a significant role in clinical assessment of cervical cancer as they get enlarged with cancer progression. In order to assess the evolution of the disease and treatment planning, automatic LN classification as benign or malignant is highly desired. In this study, we proposed a computer-aided pelvic region analysis framework using multimodal MR images to detect and classify LN as suspect or non-suspect. Our framework produced promising results, with a segmentation accuracy of 70.68% and classification accuracy of 70.21%. In our future work, we will first extend our method into a *fully-automatic and joint* LN segmentation and classification method using advanced methods such as end-to-end deep learning. Second, we will improve the DWI to T2-w MRI registration accuracy by applying pre-processing techniques on the diffusion images. Last, we will evaluate our method using a larger multimodal clinical dataset of cervical cancer.

REFERENCES

[1] World Health Organization. (2017). Comprehensive Cervical Cancer Control: A Guide to Essential Practice, 2nd edn. Geneva: WHO; 2014.

[2] Schwartz, L. H., Bogaerts, J., Ford, R., Shankar, L., Therasse, P., Gwyther, S., & Eisenhauer, E. A. (2009). Evaluation of lymph nodes with RECIST 1.1. *European journal of cancer*, *45*(2), 261-267.

[3] Chen, J., Zhang, Y., Liang, B., & Yang, Z. (2010). The utility of diffusion-weighted MR imaging in cervical cancer. *European journal of radiology*, *74*(3), e101-e106.

[4] Marks, L., Young, S., & Natarajan, S. (2013). MRI–ultrasound fusion for guidance of targeted prostate biopsy. *Current opinion in urology*, *23*(1), 43.

[5] Ahmad, S. (2014). Fusion of MRI and TRUS Images for Targeted Biopsy of Prostate. *Med Surg Urol*, *3*, e108.

[6] Stapleford, L. J., Lawson, J. D., Perkins, C., Edelman, S., Davis, L., McDonald, M. W., ... & Fox, T. (2010). Evaluation of automatic atlas-based lymph node segmentation for head-and-neck cancer. *International Journal of Radiation Oncology* Biology* Physics*, *77*(3), 959-966.

[7] Dornheim, J., Seim, H., Preim, B., Hertel, I., & Strauss, G. (2007). Segmentation of neck lymph nodes in CT datasets with stable 3D mass-spring models: Segmentation of neck lymph nodes. *Academic Radiology*, *14*(11), 1389-1399.

[8] Barbu, A., Suehling, M., Xu, X., Liu, D., Zhou, S. K., & Comaniciu, D. (2012). Automatic detection and segmentation of lymph nodes from CT data. *IEEE Transactions on Medical Imaging*, *31*(2), 240-250.

[9] Roth, H. R., Lu, L., Seff, A., Cherry, K. M., Hoffman, J., Wang, S., ... & Summers, R. M. (2014, September). A new 2.5 D representation for lymph node detection using random sets of deep convolutional neural network observations. In *International Conference on Medical Image Computing and Computer-Assisted Intervention* (pp. 520-527). Springer, Cham.

[10] Nogues, I., Lu, L., Wang, X., Roth, H., Bertasius, G., Lay, N., ... & Summers, R. M. (2016, October). Automatic lymph node cluster segmentation using holistically-nested neural networks and structured optimization in CT images. In *International Conference on Medical Image Computing and Computer-Assisted Intervention* (pp. 388-397). Springer International Publishing.

[11] Feulner, J., Zhou, S. K., Hammon, M., Hornegger, J., & Comaniciu, D. (2013). Lymph node detection and segmentation in chest CT data using discriminative learning and a spatial prior. *Medical image analysis*, *17*(2), 254-270.

[12] Zhang, Y., Ying, M. T., Yang, L., Ahuja, A. T., & Chen, D. Z. (2016, December). Coarse-to-Fine Stacked Fully Convolutional Nets for lymph node segmentation in ultrasound images. In *Bioinformatics and Biomedicine (BIBM), 2016 IEEE International Conference on*(pp. 443-448). IEEE.

[13] Kuo, J. W., Mamou, J., Wang, Y., Saegusa-Beecroft, E., Machi, J., & Feleppa, E. J. (2017). Segmentation of 3D High-frequency Ultrasound Images of Human Lymph Nodes Using Graph Cut with Energy Functional Adapted to Local Intensity Distribution. *arXiv preprint arXiv:1705.07015*.

[14] James, A. P., & Dasarathy, B. V. (2014). Medical image fusion: A survey of the state of the art. *Information Fusion*, *19*, 4-19.

[15] Gooding, M. J., Rajpoot, K., Mitchell, S., Chamberlain, P., Kennedy, S. H., & Noble, J. A. (2010). Investigation into the fusion of multiple 4-D fetal echocardiography images to improve image quality. *Ultrasound in medicine & biology*, *36*(6), 957-966.

[16] Goshtasby, A. A. (2005). *2-D and 3-D image registration: for medical, remote sensing, and industrial applications*. John Wiley & Sons.

[17] Baradarani, A., Wu, Q. J., Ahmadi, M., & Mendapara, P. (2012). Tunable halfband-pair wavelet filter banks and application to multifocus image fusion. *Pattern Recognition*, *45*(2), 657-671.

[18] Zhao, Y. Q., Wang, X. H., Wang, X. F., & Shih, F. Y. (2014). Retinal vessels segmentation based on level set and region growing. *Pattern Recognition*, *47*(7), 2437-2446.

[19] Jiang, H., He, B., Fang, D., Ma, Z., Yang, B., & Zhang, L. (2013). A region growing vessel segmentation algorithm based on spectrum information. *Computational and mathematical methods in medicine*, *2013*.

[20] Zanaty, E. A., & El-Zoghdy, S. F. (2017). A novel approach for color image segmentation based on region growing. *International Journal of Computers and Applications*, 1-17.

[21] Baghi, A., & Karami, A. (2017, April). SAR image segmentation using region growing and spectral cluster. In *Pattern Recognition and Image Analysis (IPRIA), 2017 3rd International Conference on*(pp. 229-232). IEEE.

[22] Ahuja, A. T., Ying, M., Ho, S. Y., Antonio, G., Lee, Y. P., King, A. D., & Wong, K. T. (2008). Ultrasound of malignant cervical lymph nodes. *Cancer Imaging*, *8*(1), 48.

[23] Steinkamp, H. J., Cornehl, M., Hosten, N., Pegios, W., Vogl, T., & Felix, R. (1995). Cervical lymphadenopathy: ratio of long-to short-axis diameter as a predictor of malignancy. *The British journal of radiology*, *68*(807), 266-270.